A Multimodal Approach for Comprehensive Segmentation of the Substantia Nigra

Jason Langley[1], Daniel Huddleston[2,3], Xiangchuan Chen[1], Jan Sedlacik[4], Shiyang Chen[1], and Xiaoping Hu[1]

[1]Wallace H. Coulter Department of Biomedical Engineering, Georgia Institute of Technology and Emory University, Atlanta, GA, United States, [2]Department of Neurology, Emory University, Atlanta, GA, United States, [3]Center for Health Research, Southeast, Kaiser Permanente, Atlanta, GA, United States, [4]Department of Neuroradiology, University Medical Center Hamburg-Eppendorf (UKE), Hamburg, Germany

INTRODUCTION

Degeneration of the substantia nigra (SN) is a hallmark of many neurodegenerative disorders including Parkinson's disease (PD) and Alzheimer's disease (AD). Degeneration of neuromelanin (NM) in the SN [1] and increased iron deposition in the SN [2] has been observed in both diseases. Visualization and volumetric quantification of the SN is expected to be beneficial to early detection of PD and AD as well as studying the pathogenesis of both diseases. Recent work on the visualization of the SN has focused on generating NM-sensitive contrast in the SN using a high-resolution multi-slice 2D turbo spin echo (TSE) sequence, which is sensitive to T_1-shortening effects of NM and incidental magnetization transfer contrast (MTC) effects [3-5]. However, MTC is decreased in the superior portions of the SN (see Fig. 1C) and it is probable that iron is affecting the MTC in these regions. One possible solution to this would be to add an iron sensitive modality to the segmentation procedure – namely susceptibility weighted imaging (SWI) and use SWI to delineate superior portions of the SN. A combined approach will provide more accurate delineation of the SN and improve the study of pathogenesis of PD and AD through increased sensitivity associated with iron and NM-based methods. This abstract describes a multimodal approach for SN segmentation, which combines the iron sensitivity inherent to SWI and the NM-sensitive contrast of the MTC based methods.

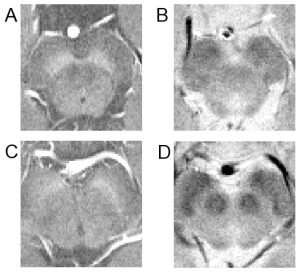

Fig. 1. A comparison of the MTC and SWI echoes. (A) & (B) display the MTC and SWI images for the same slice. As does (C) & (D), respectively.

METHODS

Data Acquisition: All experiments were performed on a 3 T scanner (TRIO, Siemens Medical Solutions, Malvern, PA) using a 12 channel transmit / receive coil. Seven normal volunteers participated in this study after obtaining informed consent in accordance with our institutional review board regulations. A dual gradient echo sequence with the following parameters was used to acquire the data: $TE_1/TE_2/TR$=2.68/20/337 ms, 15 contiguous slices, 384×312 imaging matrix, 162×200 mm (0.5×0.5×3 mm), 7 repetitions, flip angle (FA)= 40^0, MTC pulse (300^0, 1.2 kHz off-resonance, 10 ms duration), and 470 Hz/pixel receiver bandwidth.

MTC Image Processing: Magnitude data of TE_1 was averaged over all repetitions after spatial registration to the first measurement using FLIRT in the FSL software package (Oxford University, United Kingdom). The averaged images were further processed by the MTC segmentation scheme [8].

SWI Image Processing: Magnitude images of TE_2 were also averaged for all repetitions after spatial registration using FLIRT with the transformation matrices stored by the earlier MTC registration. Next, the phase data of TE_2 of each repetition was unwrapped [6] and the unwrapped phase maps were averaged after registration to the first measurement using the earlier stored transformation matrices. The resulting unwrapped phase map was high pass filtered, and used to generate phase mask, and susceptibility weighted images were created by multiplying the phase mask with the averaged structural image [7]. Phase unwrapping and filtering were performed using MATLAB.

SN Segmentation Schemes: The SN from the MTC was segmented using the method presented in [8]. For segmenting the SN from the SWI images, a region of interest (ROI) large enough to contain the SN was chosen and the SN was segmented using the following steps:

(1) Reference ROIs (circles with diameter in 5 mm) were placed in the tissues surrounding the SN for 5 consecutive slices, starting from the upper most slice containing the SN and descending 5 slices. Each slice had 2 ROIs, flanking both the left and right SN.

(2) As with the MTC echo, voxel intensities of these ROIs were verified as approximately normally distributed. The mean and standard deviation of the ROIs were calculated and a threshold $T=I_{MEAN}-3I_{SD}$ was created.

(3) Finally, voxels with intensities lower than T were added to the SN mask. The estimated SN volumes from the MTC-based and SWI-based segmentation schemes are then combined to yield the total SN volume.

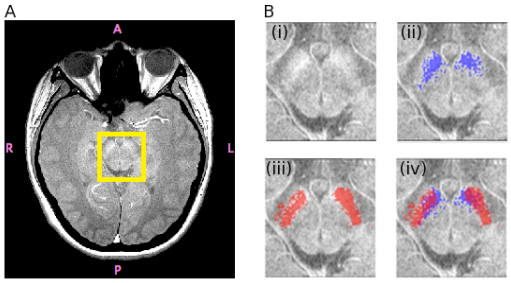

Fig. 2. **A**. An image from the MTC echo. **B**. The images in (i-iv) are zoomed in views of the PT **A**. (i) A view of the SN with no mask. (ii) Mask of the SN estimated from the MTC method (blue). (iii) Mask of the SN estimated from the SWI method (red). (iv) Masks of the SN from the MTC method (blue) and the SWI method (red) overlapped

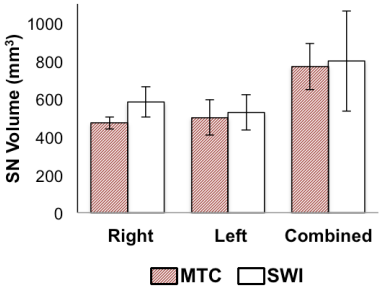

Fig. 3. A comparison of SN volumetric estimates from the MTC and SWI echoes. The overlap for each echo is ~10%.

RESULTS AND DISCUSSION

Fig. 1C shows the deficiency in MTC for superior regions of the SN when compared to the SWI echo (Fig.1D). Here, the MTC has fallen below the three standard deviations above the mean threshold set for the MTC segmentation scheme and it is not possible to delineate the SN using MTC. Whereas in inferior slices, where the susceptibility weighted contrast is minimal, the MTC echo shows higher contrast in the regions thought to be part of the SN (see Fig 1. A-B). Hence, a joint approach combining MTC and SWI for segmentation of the SN is more robust.

The average SN volumes across all subjects from the MTC and SWI echoes are 909.9±278.1 mm^3 and 770.6±122.1 mm^3, respectively (see Fig. 3). The overlap between the SN mask from the MTC echo and the SN mask from the SWI echo, defined as the cardinality of the intersection of the two masks divided by the cardinality of the union of the two masks, was quantified. The overlap for the left, right, and combined (left+right) volumes is 0.124±0.050, 0.118 ±0.039, and 0.122±0.034, respectively. A slice with the maximum overlap for a subject is illustrated in Fig. 2 (B-iv) and the mask estimated from the SWI echo is shown in red and the mask from the MTC echo is shown in blue. The low overlap between the SN volumes estimated from the MTC and SWI echoes (~12%) indicates that the two modalities are complementary in delineating the SN.

CONCLUSION

The multimodal approach is beneficial in that other structures, namely the red nucleus (RN) and subthalamic nucleus (STN), are visible on the T_2-weighted image, but not on MTC where only the grey matter, white matter, and the SN are visible. Additional benefits arise from the sensitivity to iron content inherent in the phase map and SWI as these images are sensitive to iron content. In summary, the dual echo approach combines benefits of iron and NM sensitivities associated with the SWI and NM-MRI techniques and allows for systematic study of both iron deposition and NM degeneration in PD and AD.

REFERENCES: [1] Fearnley, *et al*. Brain 114: 2283 (1991) [2] Dexter, *et al*. Brain 114:1953 (1991) [3] Sasaki, *et al*. NeuroReport 17:1215 (2006) [4] Schwarz, *et al*. Movement Disorders 26:1633 (2011) [5] Ahn, *et al*. Proc ISMRM 2012 #7561 [6] Langley, *et al*. MRI 27:1293 (2009) [7] Haacke, *et al*. MRM 52:612 (2004) [8] Chen, *et al*. Proc ISMRM 2013 #2849

ACKNOWLEDGEMENTS: This work was partially funded by William N. and Bernice E. Bumpus Foundation Early Career Investigator Innovation Award (BFIA 2011.3)